Numerical studies on the effect of electric pulses on an egg-shaped cell with a spherical nucleus

François Buret, Nicolas Faure, Laurent Nicolas, Ronan Perrussel, Clair Poignard

INRIA

INSTITUT NATIONAL DE RECHERCHE EN INFORMATIQUE ET EN AUTOMATIQUE

Numerical studies on the effect of electric pulses on an egg-shaped cell with a spherical nucleus

François Buret, Nicolas Faure, Laurent Nicolas, Ronan Perrussel — Clair Poignard

N° 7270

Avril 2010

Thème NUM

Rapport de recherche

ISSN 0249-6399 ISRN INRIA/RR--7270--FR+ENG

INSTITUT NATIONAL
DE RECHERCHE
EN INFORMATIQUE
ET EN AUTOMATIQUE

INRIA

centre de recherche
BORDEAUX - SUD OUEST

Numerical studies on the effect of electric pulses on an egg-shaped cell with a spherical nucleus

François Buret, Nicolas Faure, Laurent Nicolas, Ronan Perrussel *
, Clair Poignard†

Thème NUM — Systèmes numériques
Équipes-Projets MC2

Rapport de recherche n° 7270 — Avril 2010 — 18 pages

Abstract: In this paper, we study the influence of nanosecond electrical pulses on the phenomena arising in a biological cell model composed of a nucleus embedded in a cytoplasm, both entities being surrounded by a thin resistive membrane. The time-harmonic and the time-transient equations of the electric potential are presented, and accurate approximations of these equations are given, that avoid to mesh the thin resistive membranes. Numerical formulations of the partial differential equations are derived and simulations are performed in order to study the sensitivity of an eukaryotic cell to the orientation, the amplitude and the duration of the applied electric pulses.

Key-words: Electroporation Modelling, Finite Element Methods, Variational Formulation, Electric Potential

* Laboratoire Ampère CNRS UMR5005, Université de Lyon & École Centrale de Lyon, F-69134 Écully, France
† INRIA Bordeaux-Sud-Ouest, Institut de Mathématiques de Bordeaux, CNRS UMR 5251 & Université de Bordeaux1, 351 cours de la Libération, 33405 Talence Cedex, France

Centre de recherche INRIA Bordeaux – Sud Ouest
Domaine Universitaire - 351, cours de la Libération 33405 Talence Cedex
Téléphone : +33 5 40 00 69 00

Etude Numérique de l'effet d'un pulse électrique sur une cellule avec un noyau.

Résumé : Pas de résumé

Mots-clés : Electroporation, Eléments Finis, Formulation Variationnelle, Potentiel Electrique

Contents

1 Introduction **4**

2 Models and methods **5**
2.1 Equations of the complete cell model 5
2.1.a Time-dependent voltage potential 5
2.1.b Time-harmonic voltage potential 6
2.2 The cell model: a high contrast medium with thin layers 6
2.3 Variational method for simulations 8
2.3.a Formulation for the time-harmonic potential 8
2.3.b Formulation for the time-dependent potential 9

3 Numerical simulations by F.E.M **9**
3.1 Complements on the axisymmetric formulation 9
3.2 How to reach the nucleus? Study of the spectrum of the pulse . . 10
3.3 Sensitivity to the field orientation 13
3.3.a Time-harmonic results 13
3.3.b Time-transient simulation 14

4 Conclusion **16**

1 Introduction

Biological assemblies are sensitive to electrical perturbations. For instance, high voltage microsecond (μs) pulses can interact with living organisms, leading to modifications of the cytoplasmic membrane structures. One of these modifications, called *electropermeabilization* or *electroporation*, consists of an increase of the membrane permeability: molecules that otherwise cannot diffuse through the cell membrane do penetrate into the cell [Gabriel and Teissié(1999)]. This phenomenon is closely related to the *transmembrane potential* (TMP), which is the potential difference across the membrane: under a threshold value of the TMP, the cell membrane structure does not change, and the membrane barrier protects the cell from outer aggressions, but when the TMP overcomes this threshold value, a local destructuration of the phospholipidic bilayer occurs.

New developments are running in the fields of biotechnology and clinical drug delivery. The safe use of these approaches requires a deep knowledge of the involved space and time-dependent mechanisms. Both molecular dynamics and preliminary experimental approaches indicate that the *key steps occur at the nanosecond (ns) time scale*. Recently, Schoenbach *et al.* [Hu et al.(2005), Frey et al.(2006)] have demonstrated that electromagnetic pulses of short duration (order of 10 nanoseconds) can also modify the membranes of biological cell constituents such as the nucleus or the mitochondria without noticeably altering the cell membrane. Results from the literature show that *cancerous tumors* can be reduced in size by applying a limited number of voltage pulses with very fast rise time [Chen et al.(2004)]. The published works also demonstrate very promising potential applications of these ultra short high voltage pulses for *gene transfer*.

The aim of this paper is to present accurate numerical methods for the computation of the electric field in a cell model, composed by a nucleus embedded in the cell cytoplasm. The method is general in the sense that no geometry assumptions are needed, except that the cell membrane is at the same time thin and resistive. Since the membrane remains the same while its TMP does not reach the threshold value, we consider in this paper a linear cell model, meaning that we do not model the electropermeabilization process itself. Our study can be seen as preliminary works in order to define the most appropriate pulses for nucleus (and/or cell) membrane electropermeabilization, in particular we investigate the influence of the amplitude, the duration and the shape of the pulses, and of the relative orientation between the cell and the background electric field generated by the pulses.

We first present the generic cell model and the involved equations that describe the electric potential in the whole cell. We also propose an accurate approximation of the complete model that avoid to mesh the thin membranes: the numerical methods based on this formulation can be as accurate and more efficient than straightforward computations of the whole cell model. We then present numerical results based on this approximation. For the sake of simplicity, numerical simulations deal with 3D-axisymmetric cells: the cell cytoplasm is an ellipsoid that contains a spherical nucleus. Compared with the *in vitro* cell shapes, these geometric assumptions are relevant. Moreover since we do not suppose that the source terms have this symmetry, we emphasize that our computations are 3D simulations for a particular cell shape (and not only 3D-axisymmetric simulations).

The first numerical works are devoted to the study of the pulse spectrum in the time-harmonic regime: for a given pulse amplitude and orientation, we present which frequency is the most efficient to reach the nucleus membrane. We then present the effect of the orientation of the electric field on the membranes electropermeabilization in both time-harmonic and time-transient regimes. In particular, we show that for some orientation, the cytoplasmic membrane is permeabilized, while the nucleus membrane is not, whereas for another orientation, the electropermeabilization of both membranes can be achieved. We conclude by few remarks and future directions in the electropermeabilization modelling of cell membranes.

2 Models and methods

The cell model is composed by a *conductive cytoplasm* and a *conductive nucleus*, each being surrounded by an *insulating membrane*. At this stage, complex materials located inside the cell, as mitochondria or endoplasmic reticulum, are not modelled. The cell is embedded in a conductive bath, on which an electric field is imposed: the exposure system consists of two parallel and plane electrodes between which a conductive medium, containing the cell, is placed. Indeed, the aim is to impose an homogeneous electric field to the cell.

2.1 Equations of the complete cell model

Denote respectively by $\mathcal{O}_n$, $\mathcal{O}_c$ and $\mathcal{O}_e$ the conductive nuclear, cytoplasmic, and extracellular media, and let $\mathcal{O}_c^m$ and $\mathcal{O}_n^m$ be the respective cytoplasmic and nuclear membranes, that are resistive and thin. Let Ω be the whole domain defined by

$$\Omega = \mathcal{O}_n \cup \overline{\mathcal{O}_n^m} \cup \mathcal{O}_c \cup \overline{\mathcal{O}_c^m} \cup \mathcal{O}_e$$

Denote by σ and ε_r respectively the piecewise constant conductivity and relative permittivity of the domain Ω:

$$(\sigma, \varepsilon_r) = \begin{cases} (\sigma_e, \varepsilon_e)\,, \text{ in } \mathcal{O}_e, \\ (\sigma_c, \varepsilon_c)\,, \text{ in } \mathcal{O}_c, \\ (\sigma_n, \varepsilon_n)\,, \text{ in } \mathcal{O}_n, \\ (\sigma_m, \varepsilon_m)\,, \text{ in } \mathcal{O}_n^m \cup \mathcal{O}_c^m. \end{cases} \tag{1}$$

We denote by $\partial\Omega$ the boundary of the domain Ω and we split $\partial\Omega$ up into two disjoint parts:

$$\partial\Omega = \partial\Omega_D \cup \partial\Omega_N, \quad \partial\Omega_D \cap \partial\Omega_N = \emptyset.$$

On $\partial\Omega_D$ we impose Dirichlet boundary conditions, meaning that the electrodes are located on $\partial\Omega_D$ whereas homogeneous Neumann boundary conditions are imposed on $\partial\Omega_N$.

2.1.a Time-dependent voltage potential

Supposing that before the pulse the cell is in a steady state — *i.e.* that the potential equals 0 — the electric potential V satisfies the following partial differential equation, so-called *electro-quasistatic formulation* in the time-transient

case (the choice of this formulation is fully justified by the characteristic time constants of the different physical phenomena [Steinmetz et al.(2009)]):

$$\forall x \in \Omega,\, V\left(t=0,x\right)=0,$$

and for $t>0$,

$$\begin{cases} -\nabla.\left(\left(\varepsilon_0\varepsilon_r\dfrac{\partial}{\partial t}+\sigma\right)\nabla V\right)=0,\ \text{in } \Omega \\ V|_{\partial\Omega_D}(x,t)=V_{\text{imp}}(x,t) \text{ and } \partial_{\mathbf{n}}V|_{\partial\Omega_N}(x,t)=0, \end{cases} \tag{2}$$

where V_{imp} is enforced on the electrodes and $\mathbf{n}$ denotes the unitary outgoing normal of the domain.

2.1.b Time-harmonic voltage potential

Suppose that sinusoidal pulses are imposed to the cell, hence at steady state V_{imp} equals

$$\forall (x,t)\in\partial\Omega_D\times(0,+\infty),\quad V_{\text{imp}}(x,t)=\Re(u_{imp}(x)e^{\mathrm{i}\omega t}),$$

where ω denotes the pulses frequency. Since the considered model is linear, then V equals

$$V(x,t)=\Re(u(x)e^{\mathrm{i}\omega t}),$$

where u satisfies the following partial differential equation

$$\begin{cases} -\nabla.\left(\left(\mathrm{i}\omega\varepsilon_0\varepsilon_r+\sigma\right)\nabla u\right)=0,\ \text{in } \Omega \\ u|_{\partial\Omega_D}=u_{\text{imp}} \text{ and } \partial_{\mathbf{n}}u|_{\partial\Omega_N}=0. \end{cases} \tag{3}$$

2.2 The cell model: a high contrast medium with thin layers

From the electrical engineering point of view, biological cells are non standard materials composed of high contrast media with thin layers (see Fig. 1). More precisely, the nucleus, the cytoplasm and the extracellular conductivities are of order 1S/m, while the conductivity of the phospholipidic membranes surrounding the cytoplasm and the nucleus is small. In the S.I units, its value is about 10^{-9}S/m, which is similar to the value of the membrane thickness, that is about 10^{-9}m. The geometrical and electrical parameters of the cell considered in this work — coming from the relevant literature [Kotnik and Miklavčič(2006)] — are given in Fig. 1.

On account of such properties, straightforward naive simulations of equations (2) or (3) are time and memory consuming, and sometimes inaccurate since the matrices involved by numerical simulations are ill-conditioned especially for complex cell shapes. We emphasize that a numerical widening of the membrane is not relevant to study the transmembrane potential, since it is not a linear function of the membrane thickness, therefore accurate computations of the transmembrane potential for large membranes do not predict any results for the real thin membranes. To avoid such drawbacks, an alternative rigorous approach consists in replacing the thin resistive membranes by appropriate

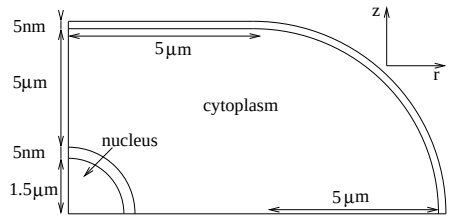

region	σ(S/m)	ε_r
nucleus cytoplasm	0.3	80
nucleus membrane	10^{-9}	5
cell cytoplasm	0.3	80
cell membrane	10^{-9}	5
exterior bath	1.2	80

Figure 1: 1/4 of the geometry of the cell considered in this work (z-axis is an axis of revolution) and its electrical parameters.

transmission conditions across the boundary of the domain they surround (see [Poignard et al.(2008), Poignard(2009), Perrussel and Poignard(2010)]). This approximation is accurate since the error is of the order of the membrane thickness, and it avoids meshing the thin membrane, leading to more precise and less costly results than naive simulations. Denote by Ω_e and Ω_c the following domains:

$$\Omega_e = \mathcal{O}_e \cup \overline{\mathcal{O}_c^m}, \quad \Omega_c = \mathcal{O}_c \cup \overline{\mathcal{O}_n^m},$$

let Γ_n be the boundary of $\mathcal{O}_n$ and denote by and Γ_c the boundary of Ω_c deprived of Γ_n. According to Fig. 1, we suppose that both cytoplasmic and nuclear membranes have the same dielectric properties and thickness. We denote by C_m and S_m the respective membrane capacitance and surface conductance that are defined by

$$C_m = \frac{\varepsilon_0 \varepsilon_m}{\delta}, \quad S_m = \frac{\sigma_m}{\delta}.$$

To simplify notations, we still denote by (σ, ε_r) the following piecewise constant functions

$$(\sigma, \varepsilon_r) = \begin{cases} (\sigma_e, \varepsilon_e)\,, \text{ in } \Omega_e, \\ (\sigma_c, \varepsilon_c)\,, \text{ in } \Omega_c, \\ (\sigma_n, \varepsilon_n)\,, \text{ in } \mathcal{O}_n. \end{cases} \tag{4}$$

The electric potential is rigorously approximated by the solution to the following problem

$$\Delta V = 0, \quad \text{in } \Omega_e \cup \Omega_c \cup \mathcal{O}_n, \quad V|_{\partial\Omega_D} = V_{imp}, \quad \partial_{\mathbf{n}} V|_{\partial\Omega_N} = 0.$$

with the following transmission conditions

$$\text{on } \Gamma_c \begin{cases} \varepsilon_0 \partial_t \left[\varepsilon_r \partial_n V\right]_{\Gamma_c} + \left[\sigma \partial_n V\right]_{\Gamma_c} = 0, \\ C_m \partial_t \left[V\right]_{\Gamma_c} + S_m \left[V\right]_{\Gamma_c} = \left(\varepsilon_0 \varepsilon_c \partial_t \partial_n V|_{\Gamma_c^-} + \sigma_c \partial_n V|_{\Gamma_c^-}\right), \end{cases} \tag{5a}$$

$$\text{on } \Gamma_n \begin{cases} \varepsilon_0 \partial_t \left[\varepsilon_r \partial_n V\right]_{\Gamma_n} + \left[\sigma \partial_n V\right]_{\Gamma_n} = 0, \\ C_m \partial_t \left[V\right]_{\Gamma_n} + S_m \left[V\right]_{\Gamma_n} = \left(\varepsilon_0 \varepsilon_n \partial_t \partial_n V|_{\Gamma_n^-} + \sigma_n \partial_n V|_{\Gamma_n^-}\right). \end{cases} \tag{5b}$$

In time-harmonic regime the amplitude of the potential is approximated by the solution to

$$\Delta u = 0, \quad \text{in } \Omega_e \cup \Omega_c \cup \mathcal{O}_n, \quad u|_{\partial\Omega_D} = u_{imp}, \quad \partial_{\mathbf{n}} u|_{\partial\Omega_N} = 0,$$

$$\text{with the conditions on } \Gamma_c \begin{cases} [(\mathrm{i}\omega\varepsilon_0\varepsilon_r + \sigma)\,\partial_n u]_{\Gamma_c} = 0, \\ (\mathrm{i}\omega C_m + S_m)\,[u]_{\Gamma_c} = (\mathrm{i}\omega\varepsilon_0\varepsilon_c + \sigma_c)\,\partial_n u|_{\Gamma_c^-}, \end{cases} \tag{6a}$$

$$\text{and similarly on } \Gamma_n \begin{cases} [(\mathrm{i}\omega\varepsilon_0\varepsilon_r + \sigma)\,\partial_n u]_{\Gamma_c} = 0, \\ (\mathrm{i}\omega C_m + S_m)\,[u]_{\Gamma_n} = (\mathrm{i}\omega\varepsilon_0\varepsilon_n + \sigma_n)\,\partial_n u|_{\Gamma_n^-}. \end{cases} \tag{6b}$$

2.3 Variational method for simulations

Approximate transmissions (5a)–(5b) or (6a)–(6b) show that the potential is discontinuous across the membranes, which is consistent with resistive thin layer properties. However these discontinuities have to be taken into account properly to obtain accurate numerical simulations. With the help of physical arguments Pucihar *et al.* present conditions [Pucihar et al.(2006)] similar to (6a)–(6b): the papers [Poignard et al.(2008), Poignard(2009), Perrussel and Poignard(2010)] quoted above can be seen as a rigorous proof (and a generalization) of these conditions. In order to solve such a problem, Pucihar *et al.* propose an iterative method that consists in expliciting the flux $(\mathrm{i}\omega\varepsilon_0\varepsilon_c + \sigma_c)\,\partial_n u|_{\Gamma_c^-}$, however this method is numerically instable, time consuming, and can lead to inaccurate results, especially for the time-transient case or when including cytoplasmic constituents. Actually, observe that the jump of the potential is given in terms of its normal derivative, and therefore this cannot be rigorously considered as a source term imposed on the surfaces Γ_c and Γ_n. We propose here a variational method that lead to a direct computation of the involved transmission conditions.

The variational framework of such formulations is described in the previous paper of Perrussel and Poignard [Perrussel and Poignard(2010)], we just present here the heuristics in order to compute efficiently the partial differential equations (P.D.E.). We suppose that the space-discretization of Ω is already performed. Since the numerical difficulties lie in the transmission conditions – the jumps of the potentials and the fluxes across the membrane – we present how to compute the rigidity matrix in the finite element method (F.E.M).

2.3.a Formulation for the time-harmonic potential

First of all, consider the time-harmonic electric potential. Denote by $(\phi_e^k)_{k=1}^{N_e}$, $(\phi_c^k)_{k=1}^{N_c}$, and $(\phi_n^k)_{k=1}^{N_n}$ the bases of finite dimensional subspaces respectively of $H^1(\Omega_e)$, $H^1(\Omega_c)$, and $H^1(\mathcal{O}_n)$, and extend these functions by 0 in the whole domain Ω. Let $N = N_e + N_c + N_n$. Therefore, the sequence of functions

$$(\psi^k)_{k=1}^N = (\phi_e^1, \cdots, \phi_e^{N_e}, \phi_c^1, \cdots \phi_c^{N_c}, \phi_c^1, \cdots, \phi_c^{N_c})$$

is a basis of a finite dimensional subspace of the space $PH^1(\Omega)$, which is the space of functions of Ω that are H^1 in Ω_e, Ω_c and in $\mathcal{O}_n$. Since Δu vanishes in

each subdomain Ω_e, Ω_c and $\mathcal{O}_n$, u can be written as:

$$u = \sum_{k=0}^{N} \alpha^k \psi^k,$$

and according to the transmission conditions (6a)–(6b) the rigidity matrix (M_{kl}) is then

$$M_{kl} = \int_\Omega \sigma \nabla\psi^k . \nabla\psi^l \, \mathrm{d}x + \int_{\Gamma_c \cup \Gamma_n} (\mathrm{i}\omega C_m + S_m) \, [\psi^k][\psi^l] \mathrm{d}\sigma.$$

2.3.b Formulation for the time-dependent potential

When dealing with the transient formulation, it is necessary to choose an appropriate scheme in order to approach the time-derivative. A particular attention has to be turned to the condition

$$C_m \partial_t \left[V\right]_{\Gamma_c} + S_m \left[V\right]_{\Gamma_c} = \left(\varepsilon_0 \varepsilon_c \partial_t \partial_n V|_{\Gamma_c^-} + \sigma_c \partial_n V|_{\Gamma_c^-}\right).$$

As in the time-harmonic regime the jump of u is linked to its normal derivative, therefore explicit scheme as Euler scheme or even RK4 scheme are restricted by a Courant-Friedrichs-Lewy (CFL) condition as described by Guyomarc'h *et al.*[Guyomarc'h et al.(2009)]. Since the characteristic length of a cell is about few micrometers, and since the pulse duration is between few nanoseconds to few microseconds, such a CFL condition is constraining. To avoid this condition it is more advisable to use implicit schemes. For instance consider the Euler implicit scheme

$$\left(\frac{C_m}{\Delta t} + S_m\right) [V^n]_{\Gamma_c} - \left(\frac{\varepsilon_0 \varepsilon_c}{\Delta t} + \sigma_c\right) \partial_n V^n|_{\Gamma_c^-} = \frac{C_m}{\Delta t} \left[V^{n-1}\right]_{\Gamma_c} + \frac{\varepsilon_0 \varepsilon_c}{\Delta t} \partial_n V^{n-1}|_{\Gamma_c^-},$$

and similarly on Γ_n. Then, the rigidity matrix of the time-discretized problem is:

$$M_{kl} = \int_\Omega \left(\frac{\varepsilon_0 \varepsilon_c}{\Delta t} + \sigma_c\right) \nabla\psi^k . \nabla\psi^l \, \mathrm{d}x + \int_{\Gamma_c \cup \Gamma_n} \left(\frac{C_m}{\Delta t} + S_m\right) [\psi^k][\psi^l] \mathrm{d}\sigma.$$

3 Numerical simulations by F.E.M

The above P.D.E. are discretized by using the *finite element method*. The space discretization have been performed by the mesh generator Gmsh (see [Geuzaine and Remacle(2009)]) and the implementation is written in C++ and it is based on the getfem++ finite element library [Renard and Pommier(2007)]. P_2-Lagrange finite elements are considered for the spatial discretization and a Crank-Nicolson scheme is used for the time-discretization.

3.1 Complements on the axisymmetric formulation

We impose an electric field to the cell — linked to the location of the electrodes — *whose relative orientation with the cell is not necessarily following the cell axis of revolution.* For the sake of simplicity, we consider a 3D-axisymmetric geometry, hence the electric field is split up into two components as described Fig. 2:

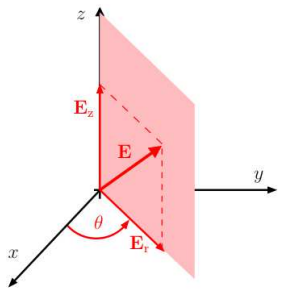

Figure 2: Field decomposition in (r, z)–coordinates: $\mathbf{E}$ is splitted up into $\mathbf{E}_r$ and $\mathbf{E}_z$.

a component along the axis of revolution $\mathbf{E}_z$ and a component along the orthogonal axis $\mathbf{E}_r$.

This geometric configuration allows to divide the computation of the potential into two disjoint bidimensional problems:

- the first problem with solution V_{z} uses the classical boundary conditions on Fig. 3(a) and the sesquilinear form (expressed in the time-harmonic case here):

$$\int_{\Omega} (i\omega\varepsilon + \sigma) \left(\frac{\partial V_{\mathrm{z}}}{\partial r} \frac{\partial v_{\mathrm{z}}}{\partial r} + \frac{\partial V_{\mathrm{z}}}{\partial z} \frac{\partial v_{\mathrm{z}}}{\partial z} \right) r dr dz + \int_{\Gamma_c \cup \Gamma_n} (\mathrm{i}\omega C_m + S_m)[V_{\mathrm{z}}][v_{\mathrm{z}}]\, r ds. \tag{7}$$

- the second problem with a solution V_{r} uses the boundary conditions on Fig. 3(b) and the sesquilinear form:

$$\begin{aligned} &\int_{\Omega} (\mathrm{i}\omega\varepsilon + \sigma) \left(\frac{\partial V_{\mathrm{r}}}{\partial r} \frac{\partial v_{\mathrm{r}}}{\partial r} + \frac{\partial V_{\mathrm{r}}}{\partial z} \frac{\partial v_{\mathrm{r}}}{\partial z} \right) r dr dz + \int_{\Omega} \frac{(\mathrm{i}\omega\varepsilon + \sigma)}{r} V_{\mathrm{r}} v_{\mathrm{r}}\, dr dz \\ &+ \int_{\Gamma_c \cup \Gamma_n} (\mathrm{i}\omega C_m + S_m)[V_{\mathrm{r}}]_{\Sigma_k}[v]_{\Sigma_k}\, r ds \end{aligned} \tag{8}$$

The electric potential is then equal to $V(r, z, \theta) = V_{\mathrm{z}}(r, z) + V_{\mathrm{r}}(r, z)\cos(\theta)$ where θ is the angular coordinate around the axis of revolution.

3.2 How to reach the nucleus? Study of the spectrum of the pulse

We first study the time-harmonic potential, for a large spectrum pulse. Since the model is linear, it is relevant to study the time-harmonic potential, since the time-transient electric voltage can be recovered by using a Fast Fourier Transform (F.F.T.) algorithm.

The frequency responses of the TMPs of the cell and of the nucleus are extracted and shown in the top of Fig. 4 when submitted to an electric field along the axis of revolution. The dashed lines describe the behavior of both nuclear and cell TMP, the solid line is the ratio of the two TMPs. The bottom of Fig. 4 shows the spectrum of pulses of respectively 10 ns and 10 μs duration:

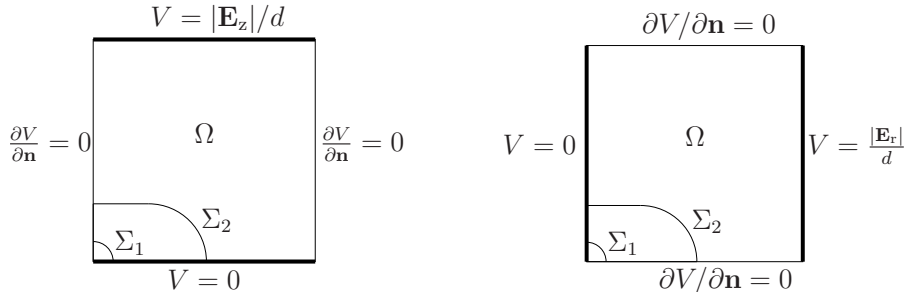

(a) $\mathbf{E}_z$. (b) $\mathbf{E}_r$.

Figure 3: Boundary conditions for the two components of the electric field. Distance d is the side length of the domain.

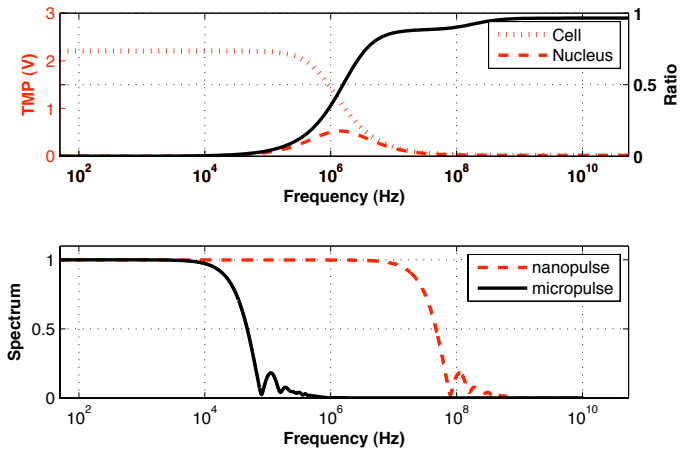

Figure 4: Time-harmonic response of the cell and normalized spectrum of ns and μs pulses. Source **E**-field: $2 \cdot 10^5$ V/m, along z-axis.

by superposing the top and bottom figures, it appears that only the ns pulse contains the frequency components to influence the nucleus.

Fig. 5 shows the scalar potential cartography and the associated electric field lines for four frequencies: 10 kHz, 1 MHz, 3 MHz and 1 GHz. For frequencies under 10 kHz the electric field does not penetrate the cell. Due to the *shielding effect* of the cell membrane it is therefore impossible to reach the nucleus. Around 2 MHz, the field penetrates the cytoplasm but still vanishes inside the nucleus. This configuration could be the most adapted to obtain the electropermeabilization of the nucleus membrane. For higher frequencies the field penetrates in the entire cell. These results show the sensitivity of the nu-

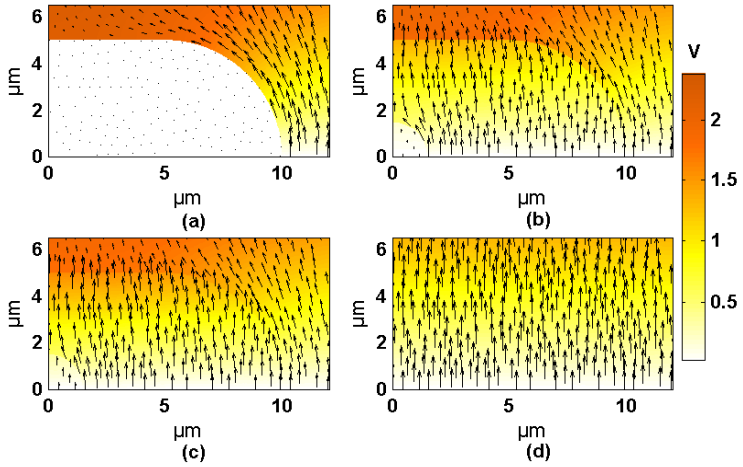

Figure 5: Time-harmonic cartography of scalar potential with electric field lines at (a) 10 kHz, (b) 1 MHz, (c) 3 MHz, (d) 1 GHz. Source **E**-field along z-axis.

cleus to a ns pulse and the feasibility of the permeabilization of the membrane of the nucleus with adapted pulse amplitude and frequency.

The qualitative analysis introduced above, based on the frequency response of the TMPs and on the spectrum of the considered pulse, can be extended with a reduced computational cost to the analysis of other pulse shapes. It should give us ideas to propose alternative pulse shapes more relevant for reaching the nucleus (or other internal contents in the cytoplasm).

Observe that according to Fig. 4, both cell and nucleus time-harmonic TMP are very smooth functions of the frequency. Therefore time-harmonic computations for few (well chosen) frequencies lead to a precise description of the TMP in the whole frequency range. Therefore the time-transient TMP can be recovered accurately by using discrete inverse F.F.T. Fig. 6 gives the value of both cellular and nuclear TMP for two types of time-transient pulses, using inverse F.F.T.

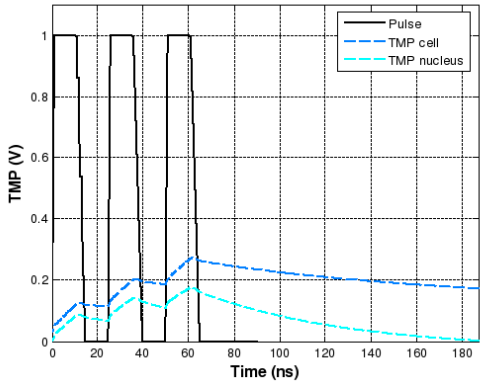

(a) pulse train at 40 MHz.

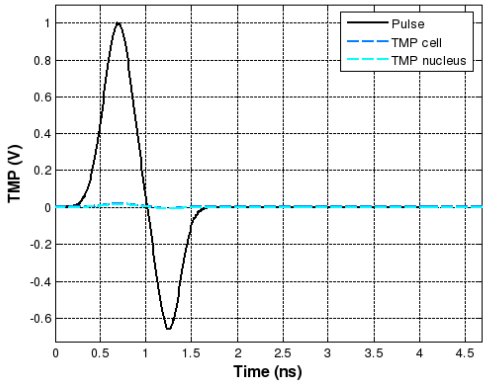

(b) Sinusodal function modulated by a Gaussian.

Figure 6: Reconstruction of the time-transient potential from time-harmonic simulations.

3.3 Sensitivity to the field orientation

In this section we investigate the influence of the field orientation on the TMP of both cell and nucleus membrane. We are confident that such study can be helpful to choose the most appropriate field orientation for a given cell shape.

3.3.a Time-harmonic results

We first study the time-harmonic regime. Fig. 7 shows the sensitivity of the TMPs to the relative orientation of the source electric field with the cell at several frequencies; let ϕ be the parameter quantifying this relative orientation, $\phi = 0^\bullet$ corresponds to the case $\mathbf{E}_\mathrm{r} = 0$ (see Fig. 3(a)) and consequently $\phi = 90^\bullet$ will correspond to the case $\mathbf{E}_\mathrm{z} = 0$ (see Fig. 3(b)). The value of the TMP on the membrane of the cell is the highest if the electrodes are perpendicular to the smallest axis of the cell, *i.e.* $\phi = 0^\bullet$, while the TMP of the nucleus is the highest if the electrodes are perpendicular to the longest axis of the cell, *i.e.*

$\phi = 90^\bullet$. Since above 10MHz the TMPs almost vanish, we emphasize that this conclusion is valid only for frequencies lower than 10 MHz.

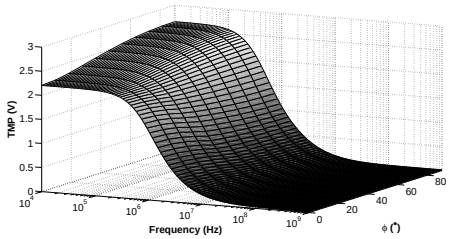

(a) TMP on the cell.

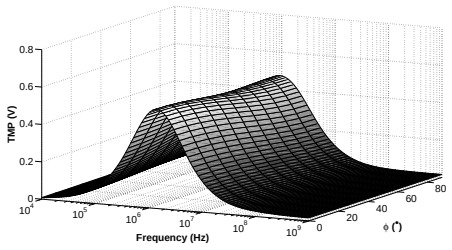

(b) TMP on the nucleus.

Figure 7: Maximal TMP on the membrane vs the orientation of the **E**-field and the frequency.

3.3.b Time-transient simulation

The cell of Fig. 1 is exposed to a pulse of 10 ns constant maximal value, of 1 ns rise time, of 4 ns fall time. Different values for the parameter ϕ were tested. Fig. 8 sums up the results obtained by showing the decrease of the TMP of the cell and of the nucleus by going from $\phi = 0^\bullet$ to $\phi = 90^\bullet$. The results of the two extreme configurations, recalled Fig. 3(a) and 3(b), are shown Fig. 9(a) and Fig. 9(b).

For each exposure configuration, the cell TMP is upper than the TMP of the nucleus. This result agree with time-harmonic results shown Fig. 4 where the ratio between the TMPs of the cell and the nucleus is less than 1, in the frequency range. The most important result is the difference in the TMP between the configuration $\phi = 90^\bullet$ and the configuration $\phi = 0^\bullet$. In the case of the cell, the increase of the TMP is around 40% while in the case of nucleus it is around 30%.

The results can explain why for a fixed amplitude of the pulse, some cells (or cell constituents such as nucleus or mitochondria) should be electroporated while others are not, depending of the orientation of each cell. This type of study may predict the amplitude and the duration of the pulse to activate the permeabilization phenomena in the membrane of the nucleus; after the activation, a more precise description of this non-linear phenomena have to be done.

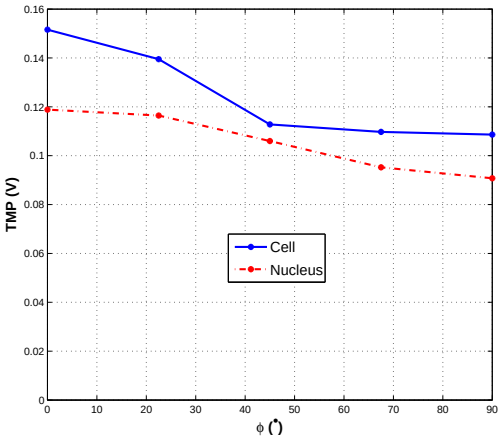

Figure 8: Maximal TMP on the membrane vs the orientation of the **E**-field.

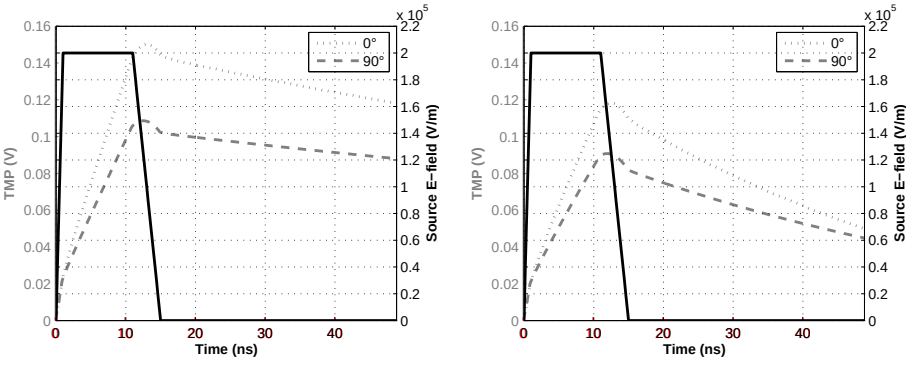

(a) TMP on the cell.

(b) TMP on the nucleus.

Figure 9: Time-transient response of the membranes to a nanopulse.

4 Conclusion

In this paper we have studied the electric potential distribution in a biological cell submitted to nanopulses or micropulses. Due to the resistive and thin membranes surrounding the cytoplasm and the nucleus a straightforward computation of the electric potential in the complete cell model lead to numerical difficulties that make *in silico* studies complex to be achieved. We have presented how to avoid such difficulties by replacing the membranes by appropriate transmission conditions, and we have presented how to implement numerically this model. In the case of a 3D-axisymmetric geometry, we have studied the influence of the pulse duration and the effect of the electric field orientation on both cell and nucleus TMPs. It appears that for a well-chosen pulse duration (or equivalently for an appropriate frequency) it is possible to increase the nuclear TMP without increasing too dramatically the cell TMP, whereas for another choice, only the cell membrane can be affected. Moreover we demonstrate that the field orientation has an influence on the TMP, and for some orientations it seems easier to reach the nucleus.

For the sake of simplicity, we assumed that the cytoplasm and the nucleus have the same dielectric properties and that their membranes are similar. We mention that for other dielectric parameters, the numerical results can be different. Since it seems difficult to obtain a very precise knowledge of the parameters, we are confident that a numerical studies of the influence of the uncertainty of the parameters on the TMPs should be performed. These study could be done as described in Voyer *et al.* [Voyer et al.(2008), Voyer et al.(2009)]. Our objective is also to incorporate non-linear electroporation effects for further study of the phenomenon as proposed in [Stewart et al.(2004), Smith et al.(2006)] for plane 2D phenomena. Using the efficiency of our numerical methods, we are confident that such approach could lead to full 3D computations and therefore it should help in understanding the electropermeabilization by nanopulses.

References

Gabriel and Teissié(1999). Gabriel, B., Teissié, J.. Time courses of mammalian cell electropermeabilization observed by millisecond imaging of membrane property changes during the pulse. *Biophys J* 1999;76:2158–2165.

Hu et al.(2005). Hu, Q., Viswanadham, S., Joshi, R.P., Schoenbach, K.H., Beebe, S.J., Blackmore, P.F.. Simulations of transient membrane behavior in cells subjected to a high-intensity ultrashort electric pulse. *Phys Rev E Stat Nonlin Soft Matter Phys* 2005;71(3 Pt 1):031914.1–031914.9.

Frey et al.(2006). Frey, W., White, J.A., Price, R.O., Blackmore, P.F., Joshi, R.P., Nuccitelli, R., Beebe, S.J., Schoenbach, K.H., Kolb, J.F.. Plasma membrane voltage changes during nanosecond pulsed electric field exposure. *Biophysical Journal* 2006;90:3608–3615.

Chen et al.(2004). Chen, N., Schoenbach, K.H., Kolb, J.F., Swanson, R.J., Garner, A.L., Yang, J., Joshi, R.P., Beebe, S.J.. Leukemic cell intracellular responses to nanosecond electric fields. *Biochemical and Biophysical Research Communications* 2004;317:421–427.

Steinmetz et al.(2009). Steinmetz, T., Kurz, S., Clemens, M.. Domains of validity of quasistatic and quasistationary field approximations. In: *Proceedings of the XV International Symposium on Theoretical Electrical Engineering (ISTET 2009)*. 2009:271–275.

Kotnik and Miklavčič(2006). Kotnik, T., Miklavčič, D.. Theoretical evaluation of voltage inducement on internal membranes of biological cells exposed to electric fields. *Biophys J* 2006;90(2):480–491.

Poignard et al.(2008). Poignard, C., Dular, P., Perrussel, R., Krähenbühl, L., Nicolas, L., Schatzman, M.. Approximate conditions replacing thin layer. *IEEE Trans on Mag* 2008;44(6):1154–1157.

Poignard(2009). Poignard, C.. About the transmembrane voltage potential of a biological cell in time-harmonic regime. *ESAIM: Proceedings* 2009;26:162–179.

Perrussel and Poignard(2010). Perrussel, R., Poignard, C.. Asymptotic Transmission Conditions for Steady-State Potential in a High Contrast Medium. A Uniform Variational Formulation for Resistive Thin Layers. Tech. Rep.; INRIA; 2010. Research Report RR-7163; URL `http://hal.inria.fr/inria-00442659`.

Pucihar et al.(2006). Pucihar, G., Kotnik, T., Valič, B., Miklavčič, D.. Numerical determination of transmembrane voltage induced on irregularly shaped cells. *Ann Biomed Eng* 2006;34(4):642–652.

Guyomarc'h et al.(2009). Guyomarc'h, G., Lee, C., Jeon, K.. A discontinuous galerkin method for elliptic interface problems with application to electroporation. *Communications in Numerical Methods in Engineering* 2009;25(10):991–1008.

Geuzaine and Remacle(2009). Geuzaine, C., Remacle, J.F.. Gmsh: A 3-D finite element mesh generator with built-in pre- and post-processing facilities. *Internat J Numer Methods Engrg* 2009;79(11):1309–1331.

Renard and Pommier(2007). Renard, Y., Pommier, J.. 2007. Getfem finite element library. `http://home.gna.org/getfem`.

Voyer et al.(2008). Voyer, D., Musy, F., Nicolas, L., Perrussel, R.. Probabilistic methods applied to 2d electromagnetic numerical dosimetry. *COMPEL: The International Journal for Computation and Mathematics in Electrical and Electronic Engineering* 2008;27:651–667.

Voyer et al.(2009). Voyer, D., Musy, F., Nicolas, L., Perrussel, R.. Comparison of methods for modeling uncertainties in a 2d hyperthermia problem. *Progress In Electromagnetics Research* 2009;11:189–204.

Stewart et al.(2004). Stewart, D., Gowrishankar, T., Weaver, J.. Transport lattice approach to describing cell electroporation: use of a local asymptotic model. *IEEE Trans on Plasma Science* 2004;32(4):1696–1708.

Smith et al.(2006). Smith, K., Gowrishankar, T., Esser, A., Stewart, D., Weaver, J.. The spatially distributed dynamic transmembrane voltage of cells and organelles due to 10 ns pulses: Meshed transport networks. *IEEE Trans on Plasma Science* 2006;34(4):1394–1404.

Centre de recherche INRIA Bordeaux – Sud Ouest
Domaine Universitaire - 351, cours de la Libération - 33405 Talence Cedex (France)

Centre de recherche INRIA Grenoble – Rhône-Alpes : 655, avenue de l'Europe - 38334 Montbonnot Saint-Ismier
Centre de recherche INRIA Lille – Nord Europe : Parc Scientifique de la Haute Borne - 40, avenue Halley - 59650 Villeneuve d'Ascq
Centre de recherche INRIA Nancy – Grand Est : LORIA, Technopôle de Nancy-Brabois - Campus scientifique
615, rue du Jardin Botanique - BP 101 - 54602 Villers-lès-Nancy Cedex
Centre de recherche INRIA Paris – Rocquencourt : Domaine de Voluceau - Rocquencourt - BP 105 - 78153 Le Chesnay Cedex
Centre de recherche INRIA Rennes – Bretagne Atlantique : IRISA, Campus universitaire de Beaulieu - 35042 Rennes Cedex
Centre de recherche INRIA Saclay – Île-de-France : Parc Orsay Université - ZAC des Vignes : 4, rue Jacques Monod - 91893 Orsay Cedex
Centre de recherche INRIA Sophia Antipolis – Méditerranée : 2004, route des Lucioles - BP 93 - 06902 Sophia Antipolis Cedex

Éditeur
INRIA - Domaine de Voluceau - Rocquencourt, BP 105 - 78153 Le Chesnay Cedex (France)
http://www.inria.fr
ISSN 0249-6399